Large Amplitude Shock-Wave Motion in Two-Dimensional, Transonic Channel Flows

T. C. Adamson Jr.,* A. F. Messiter,† and M. S. Liou‡
The University of Michigan, Ann Arbor, Mich.

Two-dimensional unsteady transonic channel flow with a shock wave is considered for the slowly varying time regime. Pressure oscillations, introduced downstream of the shock wave, cause the shock wave to oscillate; the case considered is that where the shock moves upstream to the throat, disappears, and then reappears as the downstream pressure first increases and then decreases. The subsequent shock-wave motion consists of oscillations either about the throat or about the original steady flow shock position, depending upon the values of various parameters. These two cases and the dividing case are illustrated with example calculations.

Introduction

RECENT papers on unsteady transonic channel flows, where the unsteadiness arises as a result of pressure oscillations introduced downstream of a shock wave, either have dealt with relatively small amplitude shock oscillations[1,2] or have included only very brief discussions of possible large amplitude oscillations.[3] Thus, if the channel half-width at the throat is $\bar{L}$ (overbars denote dimensional quantities), $\bar{a}^*$ is the critical sound speed, and ϵ is a small parameter which measures the typical difference between the fluid velocity and the sound speed, the case where the impressed pressure oscillations have amplitude $O(\epsilon^2)$ with a period $O(\epsilon^{-1})$ and the amplitude of the shock-wave oscillation is $O(\epsilon)$ is covered in Ref. 1; solutions are presented for a symmetric channel. In Ref. 2, where a relatively highly curved asymmetric channel is considered, the impressed pressure oscillations have amplitude $O(\epsilon^2)$ and now a period of $O(\epsilon^{-2})$, so the amplitude of the shock oscillations is $O(1)$. However, only a relatively small amplitude is actually considered, the emphasis being on asymmetry of the flow. Finally, in Ref. 3, several combinations of the impressed pressure amplitude and period are discussed, and it is pointed out by means of a simple example that it is possible to analyze the case where the shock wave moves upstream to the throat, disappears, and then later reappears. In each of the previously named references, a "slowly varying" time regime is considered, where if the characteristic time associated with the imposed flow distribution is $O(\bar{T}_{ch})$, then $\bar{T}_{ch} \gg \bar{L}/\bar{a}^*$, where $\bar{L}/\bar{a}^*$ can be regarded as a characteristic flow time.

The present paper is concerned with the case where the pressure oscillation has amplitude $O(\epsilon^2)$ and period $O(\epsilon^{-2})$, again in the slowly varying time regime, so that, as will be seen, the shock-wave oscillation amplitude is $O(1)$. In particular, we consider those cases where, as a result of the pressure oscillations introduced downstream, the shock wave moves upstream of the throat, disappears, and then reappears as the downstream pressure decreases. Then, depending upon the flow parameters, it will be shown that the subsequent shock motion will follow one of several different paths, ranging from an oscillation in which the shock disappears and reappears on a periodic basis to a periodic oscillation during which the shock never again reaches the throat. The possible applications to unsteady flow problems in inlets and flows between blades in turbomachinery indicate that the solutions to be presented for simple boundary shapes will be quite helpful toward understanding flows in more complex geometries.

Received Nov. 14, 1977; presented as Paper 78-247 at the 16th AIAA Aerospace Sciences Meeting, Huntsville, Ala., Jan. 16-18; revision received June 19, 1978.

Index categories: Nonsteady Aerodynamics; Nozzle and Channel Flow; Transonic Flow.

*Professor of Aerospace Engineering. Associate Fellow AIAA.
†Professor of Aerospace Engineering. Member AIAA.
‡Presently, Research Scientist, Flight Sciences Dept., McDonnell Douglas Research Laboratories, St. Louis, Mo. Member AIAA.

Derivation of Equation for Shock-Wave Position

The flow to be studied is an unsteady transonic flow, with a shock wave, in a symmetric two-dimensional channel. Coordinates x and y, with corresponding velocity components u and v, are parallel and perpendicular to the channel axis, respectively. The flow upstream of the wave is steady; pressure oscillations are impressed upon the flow downstream of the shock, at $x=X$, say, and cause the shock wave to oscillate. The gas is assumed to follow the perfect gas law and to have constant specific heats. The flow upstream of the shock wave is isentropic, and because the flow is transonic, the shock is weak enough that a velocity potential may be used to the order desired. The coordinates x and y are made dimensionless with respect to $\bar{L}$, time T with respect to $\bar{L}/\bar{a}^*$, and velocities with respect to $\bar{a}^*$; hence, the dimensionless velocity potential is referred to the product $\bar{L}\bar{a}^*$. The pressure P, density ρ, and temperature $\bar{T}$, are made dimensionless with respect to their critical values, and enthalpy is referred to $\bar{a}^{*2}$.

The wall shapes considered are written as follows for symmetric channels:

$$y_w = \pm\,(1+\epsilon^2 f(x)) \tag{1}$$

where $f(x)$ is the arbitrary wall shape function, such that $f(0)=f'(0)=0$. Thus, x is measured from the channel throat. The radius of curvature of the channel at the throat is $O(\epsilon^{-2})$ from Eq. (1), and as will be seen later, $u-1=O(\epsilon)$; for transonic flow $\epsilon \ll 1$.

Certain general features of the flow are determined by the relative order of the characteristic time associated with the impressed disturbances, $\bar{T}_{ch}$, and the characteristic time associated with an acoustic wave traveling through the channel, $\bar{L}/\bar{a}^*$. As mentioned previously, the slowly varying time regime is considered here, where $\bar{T}_{ch} \gg \bar{L}/\bar{a}^*$. Therefore, a parameter τ is introduced and a new stretched time coordinate is made nondimensional with $\bar{T}_{ch}$ as follows:

$$\tau \equiv \bar{T}_{ch}/(\bar{L}/\bar{a}^*) \tag{2a}$$

$$T = \tau t \tag{2b}$$

where $\tau \gg 1$ and $t=O(1)$. The relationship between τ and ϵ depends upon the case considered. Since $u-1=O(\epsilon)$, the

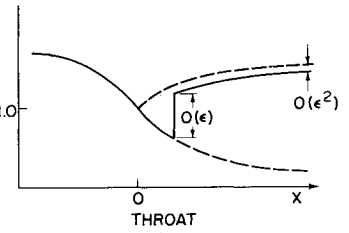

Fig. 1 Pressure distribution in nozzle with accelerating flow; --- shockless flow; —— flow with a shock wave.

time $\bar{T}_{sh}$ required for a signal to travel upstream from the origin of the flow disturbance to the shock wave is $O(\bar{L}/\bar{a}^*\epsilon)$; therefore $\bar{T}_{ch}/\bar{T}_{sh}=O(\epsilon\tau)$. If $\tau=O(\epsilon^{-1})$, the case studied in Ref. 1, then $\bar{T}_{sh}=O(\bar{T}_{ch})$ and there is a lag between the impressed oscillations in pressure and the pressure, temperature, etc., oscillations in the channel flow downstream of the shock. If $\tau=O(\epsilon^{-2})$, the case studied here and in Ref. 2, pressure signals from downstream of the shock wave reach the shock "instantaneously" in comparison with the period of the impressed changes in pressure; i.e., $\bar{T}_{sh}/\bar{T}_{ch}=O(\epsilon)$. Thus, we write:

$$\tau=(k\epsilon^2)^{-1} \tag{3}$$

where k is an arbitrary constant of order unity.

The general method of solution follows that used in Refs. 1 and 2. The solutions for u,v,P,ρ, and $\tilde{T}$ are written in the form of asymptotic expansions for $x,y,t=O(1)$. Since the flow upstream of the shock is steady and the impressed pressure downstream of the wave has time variations only in second-order terms, then to first order [i.e., $O(\epsilon)$], the entire flow is steady and the time dependence enters only in second-order terms. As shown previously[1,2] and as illustrated in Fig. 1, variations in pressure of order ϵ^2 at $x=X$ are sufficient to cause local pressure variations of order ϵ across the shock. As will be seen, these variations are also sufficient to cause shock-wave displacements of order one. Hence, relatively small impressed pressure variations can cause large local pressure changes over a large part of the channel; this, of course, is a very important element in the study of blade flutter in transonic turbomachinery.

The only difference between the problem considered in Ref. 1 and that studied here is that in Ref. 1 (hereafter referred to as case 1) $\tau=O(\epsilon^{-1})$, whereas in the present case $\tau=O(\epsilon^{-2})$; i.e., the characteristic time associated with the impressed disturbance is one order larger in the present case. Hence, in the general governing equations, since

$$\frac{\partial}{\partial T}=\frac{1}{\tau}\frac{\partial}{\partial t}$$

the partial derivatives with respect to time will be one order smaller than in case 1. Therefore, the general outer solutions may be derived easily from the outer solutions given in Ref. 1, where the word "outer" refers to those solutions valid outside a thin region enclosing the shock wave. Because the solutions in question do not satisfy the shock-wave jump conditions in second order, it is necessary here also to consider an inner region about the shock, in which the solutions satisfy the jump conditions at the shock and match with the outer solutions in the appropriate limit as the outer regions are approached. Then the inner and outer solutions can be joined to form a composite solution uniformly valid to $O(\epsilon^2)$ everywhere in the channel. Because the thickness (in the x direction) of the inner region is $O(\epsilon^{1/2})$, and in case 1 the amplitude of the shock-wave motion is $O(\epsilon)$, it is possible in case 1 to consider a stationary inner region. In the present case, the inner region thickness is again $O(\epsilon^{1/2})$, but the amplitude of the wave motion is $O(1)$ and a moving inner region must be accounted for. However, because $\tau=O(\epsilon^{-2})$, it can be shown[4] that the inner solutions are unchanged in form from those given in Ref. 1. In case 1, the shock wave remains close to a steady-state location and the relative velocity ahead of the shock wave is constant to first order, whereas in the present case the shock wave may move throughout the channel, and the upstream fluid velocity relative to the shock depends on the shock position and is thus a function of time. Since, to the order considered, no time derivatives remain in the differential equations for the inner region, the form of the solutions is the same in the two cases, the time dependence arising through the boundary conditions on the relative upstream velocity.

In view of the preceding remarks, it is seen that the general form of the composite solution holds for either case 1[1] or the present case. These solutions are repeated here, from Ref. 1, for convenience:

$$u=1+\epsilon u_1+\epsilon^2 u_2+\ldots \tag{4a}$$

$$v=\epsilon^2 v_2+\ldots \tag{4b}$$

$$P=1-\epsilon\gamma u_1-\epsilon^2\gamma u_2+\ldots \tag{4c}$$

$$\rho=1-\epsilon u_1-\epsilon^2\left(u_2+\left(\frac{\gamma-1}{2}\right)u_1^2\right)+\ldots \tag{4d}$$

$$\tilde{T}=1-\epsilon(\gamma-1)u_1-\epsilon^2(\gamma-1)\left(u_2+\frac{u_1^2}{2}\right)+\ldots \tag{4e}$$

where $\gamma=C_p/C_v$ is the ratio of the specific heats and where

$$u_1=\pm\sqrt{\frac{2}{(\gamma+1)}f(x)+C_w} \tag{5a}$$

$$u_2=f''\frac{y^2}{2}+h_x+\zeta^*_{x^*} \tag{5b}$$

$$v_2=f'y+\epsilon^{1/2}\zeta^*_y \tag{5c}$$

$$\zeta^*=\frac{4f_0''[(\gamma+1)C_u]^{1/2}}{\pi^3}\sum_{n=1}^{\infty}\frac{(-1)^n}{n^3}\cos(n\pi y)$$

$$\cdot\exp\{-n\pi x^*/[(\gamma+1)C_u]^{1/2}\} \tag{5d}$$

$$x^*=(x-x_{s0})\epsilon^{-1/2} \tag{5e}$$

In Eqs. (5a), C_w is an arbitrary constant determined by the value of the velocity at the throat; i.e., if the flow is supersonic or subsonic there, then $C_w>0$, but if the flow accelerates from subsonic to supersonic speed and is therefore sonic at the throat, $C_w=0$. Also, in Eqs. (5), $f'=df/dx$, etc., and f_0' is the value of f' at x_{s0}, the zero-order approximation to the shock-wave location x_s, which is expanded as:

$$x_s=x_{s0}(t)+\epsilon x_{s_1}(t)+\ldots \tag{6}$$

For case 1, $x_{s0}=\text{const}$, and in both cases, the y dependence of x_s occurs in higher order terms. In Eqs. (5b) and (5c), the function $\zeta^*(x^*,y)$ is the contribution to the composite potential function from the inner solution. Upstream of the shock wave $\zeta^*=0$, and downstream ζ^* is given by Eq. (5d). Finally, C_u is the value of u_1 at x_{s0}, evaluated upstream of the shock [upper sign in Eq. (5a)]. In case 1, $C_u=\text{const}$, while in the present case, C_u is a function of time since $x_{s0}=x_{s0}(t)$.

Before Eqs. (5) can be evaluated, it is necessary to find h_x. The equation for h_x is found from the next higher order term in v, i.e., v_3, which satisfies the boundary condition that the flow remain tangent to the channel walls. For case 1, the differential equation for h is[1]:

$$[2k_1/(\gamma+1)]h_t+u_1h_x=-u_1(f''+(2\gamma-3)u_1^2)/6+A(t) \tag{7}$$

where subscripts t and x indicate partial differentiation. In Ref. 1, a general numerical procedure for finding h_x was given, which permitted $u_1 = u_1(x,t)$. In Ref. 3, it was shown that if $u_1 = u_1(x)$, the condition finally considered in Ref. 1 and also considered here, then for case 1 ($\tau_1 = (k_1\epsilon)^{-1}$) the solution for h_x can be written as:

$$h_x = -\frac{1}{6}[f'' + (2\gamma - 3)u_1^2] + \frac{C_2}{u_1} + \frac{1}{u_1}G(t - t_\ell) \tag{8a}$$

$$t_\ell = t_\ell(x) = \int_X^x (2k_1/(\gamma+1)u_1(\xi))\,d\xi \tag{8b}$$

In Eq. (8a), C_2 is an arbitrary constant of integration set by boundary conditions upstream and downstream of the shock, and $G(t)$ is proportional to the oscillation in pressure impressed downstream of the shock wave at $x = X$. That is, from Eqs. (4c, 5a, and 5b), it is seen that, as mentioned previously, the pressure varies with time in second order, and that at $x = X$, $G(t)$ is the time-varying part of h_x and thus of the pressure.

For the present case, where $\tau = O(\epsilon^{-2})$, h_t is dropped from Eq. (7) and the solution is simply Eq. (8a) with $t_\ell = 0$. That is, there is no lag between the impressed oscillations in pressure and velocity and the corresponding oscillations anywhere in that part of the flowfield affected by the impressed oscillations (between the shock position x_s and X). Signals travel upstream instantaneously in comparison with the period of the oscillation.

Finally, it is possible to calculate the shock position as a function of time. First, we consider the shock-wave velocity, $u_s = dx_s/dT + O(\epsilon^3)$; ($v_s = O(\epsilon^{7/2})$ is negligible).[1] Relative to the shock wave, the first-order shock jump condition is, for transonic flow, $(u_1 - u_{1s})_d = -(u_1 - u_{1s})_u$, where u_{1s} is the first-order absolute shock-wave velocity (i.e., $u_s = \epsilon u_{1s} + \epsilon^2 u_{2s} + \ldots$) and where the subscripts u and d refer to conditions immediately upstream and downstream of the shock, respectively. Now, u_{1u} and u_{1d} are given by Eq. (5a) with the upper and lower sign, respectively, so $u_{1d} = -u_{1u}$, and from the shock relations, therefore, $u_{1s} = 0$. Since the shock jump conditions are not satisfied by u_2, it is clear that $u_{s2} \neq 0$ and so $u_s = O(\epsilon^2)$. Therefore,

$$u_s = \frac{dx_s}{dT} = k\epsilon^2 \frac{d}{dt}(x_{s0} + \epsilon x_{s1} + \ldots) = O(\epsilon^2) \tag{9}$$

and $x_{s0} = x_{s0}(t)$. This means that the lowest order term in x_s varies with time so that the amplitude of the shock motion is $O(1)$. For the shock motion in case 1, $\tau = O(\epsilon^{-1})$ and $u_s = O(\epsilon^2)$, so that $x_{s0} = \text{const}$, $x_{s1} = x_{s1}(t)$, and the shock wave undergoes only small displacements from its equilibrium position.[1]

The governing equation for $x_{s0}(t)$, the first approximation to the instantaneous shock position, is derived by applying the mass conservation principle to a control volume containing (moving with) the shock wave. The change in entropy across the wave ($O(\epsilon^3)$) is employed in writing the density downstream of the wave. Although variations in ρ and u up to third order must therefore be considered, the final result involves only second-order terms, a result reported previously.[1,2,5] Details of the calculations are given in Ref. 4; the resulting equation for $u_{s2} = k\,dx_{s0}/dt$ is:

$$\frac{4k}{(\gamma+1)}\frac{dx_{s0}}{dt} = h_{xd} + h_{xu} + \frac{f_0''}{3} - C_u^2 \tag{10}$$

This equation has exactly the same form as that given for case 1 (Ref. 1), the only difference being that for case 1 dx_{s1}/dt is calculated; in the present case, $C_u = C_u(t)$, whereas in case 1, $C_u = \text{const}$. For the specific problem considered here, where the flow upstream of the shock is steady and pressure oscillations are impressed upon the flow downstream of the shock at $x = X$, say, h_{xu} is given by Eq. (8a) evaluated at $x = x_{s0}$, with $G = 0$. For a flow which is sonic at the throat (e.g., an accelerating flow), the case considered here, $C_{2u} = 0$ also. Again, subscripts u and d denote conditions immediately upstream and downstream of the shock wave, respectively. Equation (8a), evaluated at x_{s0}, is used for h_{xd} (with $t_\ell = 0$ for the present case); the value chosen for C_{2d} gives the steady-state location for the shock wave when $G(t) = 0$. Thus, if the above mentioned relations for h_{xu} and h_{xd} are substituted into Eq. (10), one finds that

$$\frac{4k}{(\gamma+1)}\frac{dx_{s0}}{dt} = -\frac{1}{C_u}\left[C_{2d} + \frac{2\gamma}{3}C_u^3 + G(t)\right] \tag{11}$$

Hence, at the steady-state shock location, where $G(t) = 0$ and $dx_{s0}/dt = 0$, $C_{2d} = -2\gamma\, C_u^3(x_{s0})/3$, where x_{s0} is now a constant. Thus, setting C_{2d} gives $C_u(x_{s0})$, which from Eq. (5a) means that the steady-state value of x_{s0} can be calculated for a given wall shape. If we denote by C_{u0} the value of C_u at this steady-state location, then Eq. (11) can be written as follows:

$$\frac{4k}{(\gamma+1)}\frac{dx_{s0}}{dt} = \frac{1}{C_u}\left[\frac{2\gamma}{3}(C_{u0}^3 - C_u^3) - G(t)\right] \tag{12}$$

Integrating this equation thus gives the unsteady shock location measured from the steady flow location, for a given arbitrary impressed pressure oscillation represented by $G(t)$.

Before analyzing the shock motion, it is of interest to note that it is possible to write a generalized solution valid for either case 1, with $\tau = O(\epsilon^{-1})$, or for the present case, with $\tau = O(\epsilon^{-2})$. Thus, if one replaces Eq. (8b) with the following generalized relation,

$$t_\ell = \frac{1}{\tau\epsilon}\int_X^x \frac{2}{(\gamma+1)}\frac{d\xi}{u_1(\xi)} \tag{13}$$

and Eq. (11) with the following equations

$$\frac{1}{\tau\epsilon^2}\frac{4}{(\gamma+1)}\frac{dx_s^+}{dt} = -\frac{1}{C_u}\left[C_{2d} + \frac{2\gamma}{3}C_u^3 + G(t - t_{\ell 0})\right] \tag{14a}$$

$$x_s = x_0 + x_s^+(t) \tag{14b}$$

then the general solution is given by Eqs. (4, 5, 8a, 13, and 14). In Eqs. (14), x_0 is the steady-state location of the shock and $t_{\ell 0} = t_\ell(x_0)$. It is seen that for $\tau = O(\epsilon^{-1})$, then from Eq. (13), $t_\ell = O(1)$, and from Eq. (14a), $x_s^+ = O(\epsilon)$, i.e., $x_s^+ = \epsilon x_{s1}$. For $\tau = O(\epsilon^{-2})$, then $\tau_\ell = O(\epsilon)$ and is negligible, and $x_s^+ = O(1)$, so $x_s^+ + x_0 = x_{s0}$. The generalized solutions are particularly useful in making numerical calculations; it is easy to separate case 1 and the present case asymptotically, but it is not easy to choose one case over the other in a given physical situation, i.e., with given numerical values of ϵ and τ.

Large Amplitude Shock-Wave Motion

As indicated previously, when $\tau = O(\epsilon^{-2})$ the shock-wave motion resulting from pressure oscillations impressed downstream of the shock wave has an amplitude of order unity. As a result, there are conditions under which the shock will move upstream through the nozzle, disappear upstream, and then reappear as the downstream plenum pressure drops to the point where a shock wave in the channel is necessary to satisfy this instantaneous pressure requirement. The conditions for this occurrence and the subsequent shock-wave motion depend in a complex manner upon the forcing function G, the steady-state shock position represented by C_{2d}, the walk shape $f(x)$, and the numerical value of the time constant, represented by k.

The equation which governs the shock motion is Eq. (11) or (12), where, since $x_s = x_{s0} + O(\epsilon)$, to the order considered here

x_s and x_{s0} are interchangeable. It is interesting to note that although signals from the impressed disturbances reach the shock wave instantaneously in a first approximation, the shock wave does not move in phase with this disturbance. The shock velocity is finite, and indeed there is a lag between the impressed disturbance $G(t)$ and the resulting shock velocity dx_{s0}/dt. In Eq. (12), for example, it is seen that the term $(C_{u0}^3 - C_u^3)$ always has a sign such that its effect is to cause the shock to move toward the equilibrium or steady-state position. On the other hand, $G(t)$ is a forcing function which changes sign periodically. The result is a shock motion which lags $G(t)$.

It is clear from Eq. (11) or (12) that singularities occur as the shock wave approaches the throat, where $C_u \to 0$. The behavior of integral curves near the throat can be found if Eq. (11) is written for x_{s0} (and thus C_u) small compared to unity and for $|t-t_0| \ll 1$, where t_0 is the value of t at which the bracket on the right-hand side of Eq. (11) goes to zero at the throat, $x_{s0}=0$. Thus, if, for example,

$$G = G_0 \sin bt \tag{15}$$

then

$$\sin bt_0 = -C_{2d}/G_0 \tag{16}$$

and Eq. (11) becomes, for $x_{s0} \ll 1$ and $|t-t_0| \ll 1$,

$$\frac{dx_{s0}}{dt} = -\frac{(\gamma+1)}{4k}(bG_0 \cos bt_0)\left(\frac{t-t_0}{C_u}\right) \tag{17a}$$

$$\cos bt_0 = \pm\sqrt{1-(C_{2d}/G_0)^2} \tag{17b}$$

where, again, $C_u = u_{1u}(x_{s0})$ is the value of u_1 at $x = x_{s0}(t)$ upstream of the shock, and where $C_u^3 \ll |t-t_0|$. A typical wall shape and the corresponding solution to Eq. (17a) are, in the neighborhood of the throat,

$$f(x) = ax^2 \tag{18a}$$

$$x_{s0}^2 = -\frac{(\gamma+1)^{3/2}}{2^{5/2}k}\frac{b}{\sqrt{a}}G_0(\cos bt_0)(t-t_0)^2 + C \tag{18b}$$

where C is a constant. Thus, if $\cos bt_0 > 0$, the point $(0,t_0)$ is a center and the integral curves (ellipses) in the neighborhood of this center cross $x_{s0}=0$ with an infinite slope. On the other hand, if $\cos bt_0 < 0$, the integral curves in the neighborhood of $(0,t_0)$ are hyperbolas, the point being a saddle point, and the two integral curve pass through the point $(0,t_0)$ with slopes

$$\frac{dx_{s0}}{dt} = \pm\left\{\frac{(\gamma+1)^{3/2}}{2^{5/2}k}\frac{bG_0}{a^{1/2}}|\cos bt_0|\right\}^{1/2} \tag{19}$$

An understanding of the possible shock motions may be gained by analyzing the integral curves which pass through the saddle points. The three possible configurations for these curves are sketched in Fig. 2. In these sketches, the arrows indicate the direction the solutions must follow as time increases. In Fig. 2a, conditions are such that the integral curves entering the saddle point (indicated by x) originate from a particular $x_{s0}=x_0$ at $t=0$. Those leaving the saddle begin to rise, then reverse their directions and cross the time axis with vertical slope at some point between the center (indicated by •) and the next saddle point. Other integral curves are also sketched, as dotted lines. As indicated in the sketch, the paths traced by the integral curves are repetitive. In Fig. 2c, the opposite situation exists; the integral curves entering the saddle point begin on the axis between a saddle and a center with an infinite slope and then change direction and enter the next saddle point. Those curves leaving the saddle never return to the axis $x_{s0}=0$, but asymptotically approach a single periodic curve (for a given C_{2d}). Those curves which originate

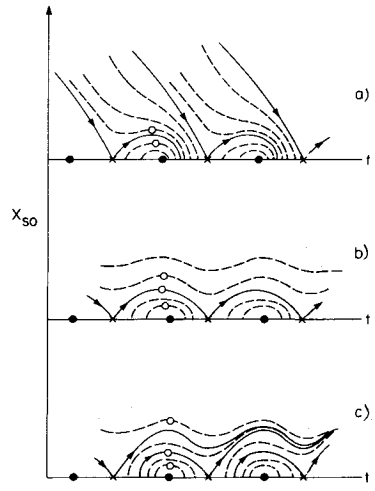

Fig. 2 Sketch of possible configurations for integral curves through saddle points, (—); other integral curves (---); •, center; x, saddle point. a) Integral curves leaving x reach time axis before next x; b) integral curves leaving x reach time axis at next x; c) integral curves leaving x never return to time axis.

with an x_{s0} greater than any x_{s0} on this periodic curve will approach the periodic curve asymptotically from above. In the dividing case, shown in Fig. 2b, the curves entering and leaving the saddle points are the same curve.

The integral curve map obtained in any given case depends upon C_{2d}, k, $G(t)$, and the wall shape $f(x)$. Although general solutions from which a general criterion for the dividing condition (Fig. 2b) could be derived are not available, an approximate result can be found for G as given in Eq. (15) and $f(x)$ as in Eq. (18a). Then, Eq. (11) becomes

$$Kx_{s0}\frac{dx_{s0}}{dt} = -C_{2d} - \Gamma x_{s0}^3 - G_0 \sin bt \tag{20a}$$

$$K = \frac{2^{5/2}k\sqrt{a}}{(\gamma+1)^{3/2}} \tag{20b}$$

$$\Gamma = \frac{2\gamma}{3}\left(\frac{2a}{\gamma+1}\right)^{3/2} \tag{20c}$$

and the slopes of the integral curves at the saddle points are given by Eq. (19), with t_0 and G_0 related as in Eq. (16). Now, if it is assumed that the integral curve which passes through the saddle point at $bt = bt_0$ and also through the next saddle point at $bt = bt_0 + 2\pi$ (e.g., see Fig. 2b) is approximately symmetric about $bt = bt_0 + \pi$, then the maximum value of x_{s0} is, from Eq. (20a),

$$(x_{s0})_m = (-2C_{2d}/\Gamma)^{1/3} \tag{21}$$

Next, if Eq. (20a) is integrated first over one period (e.g., $bt = bt_0$ to $bt = bt_0 + 2\pi$) and then over a half period, and since $x_{s0}=0$ at bt_0 and $bt_0 + 2\pi$ and $x_{s0} = (x_{s0})_m$ at $bt = bt_0 + \pi$, one finds the following relations:

$$0 = C_{2d} + \Gamma\int_0^{\tilde{t}} x_{s0}^3 d\tilde{t} \tag{22a}$$

$$\tilde{t} = b(t-t_0)/2\pi \tag{22b}$$

$$\frac{K(x_{s0})_m^2}{2} = -2\frac{G_0}{b}\cos bt_0 \tag{22c}$$

where, in Eq. (22c), advantage has been taken of the fact that the integral of x_{s0}^3 over half a period is half the integral over a

full period because of the symmetry of x_{s0}. Substituting for $\cos bt_0$ using Eq. (16), one finds from Eq. (22c) the following relation for G_0 for the special case (Fig. 2b):

$$(G_0^2 - C_{2d}^2)^{1/2} = bK(x_{s0})_m^2/4 \tag{23}$$

where K is given in Eq. (20b). Although this equation is useful in setting a first approximation for G_0, a more accurate result may be found by taking into account the fact that the integral curve in question is not in fact symmetric but is slightly asymmetric. In this calculation, it is necessary to employ an approximate form for $x_{s0}(t)$; a cubic equation of the following form suffices:

$$x_{s0} = C_1\tilde{t}(1-\tilde{t}) + C_2\tilde{t}(1-\tilde{t}^2) \tag{24}$$

Now, at $x_{s0} = (x_{s0})_m$, where $dx_{s0}/d\tilde{t} = 0$, $\tilde{t}$ is defined as $\tilde{t}_m$. Thus, say

$$\tilde{t}_m = \tfrac{1}{2} + \delta \tag{25}$$

It is assumed that due to the small asymmetry δ is numerically small enough that terms involving δ^2 may be ignored. Then, from Eq. (20a) evaluated at $x_{s0} = (x_{s0})_m$, Eq. (22a) with Eq. (24) used in the evaluation of the integral, Eq. (20a) integrated over one half period ($\tilde{t} = 0$ to $\tilde{t} = \frac{1}{2}$) with Eq. (24) used in integrating the x_{s0}^3 term, $(x_{s0})_m$ evaluated using Eq. (24), and Eq. (25), one can derive the following relations for $(x_{s0})_m$, δ, and finally, G_0:

$$(x_{s0})_m = (-35C_{2d}/16\Gamma)^{1/3} \tag{26a}$$

$$\delta = 3C_{2d}/8\pi bK(x_{s0})_m^2 \tag{26b}$$

$$(G_0^2 - C_{2d}^2)^{1/2} = \frac{bK(x_{s0})_m^2}{4} - \delta\pi(0.207\Gamma(x_{s0})_m^3 - C_{2d}) \tag{26c}$$

where, again, K and Γ are defined in Eqs. (20b) and (20c).

Example calculations of the integral curves through the saddle points, with the sinusoidal forcing function given in Eq. (15) and with parabolic walls as in Eq., (18a), are shown in Fig. 3. The first approximation to the special value of G_0 for case (b), calculated using Eq. (26c), must be modified using trial and error. The calculations were carried out by numerically integrating Eq. (20a), using Eq. (19) to find an initial condition near $x_{s0} = 0$. In the calculation, $b = 2$, $k = 1$, $a = (\gamma+1)/2 = 1.2$, $x_0 = 1.5$, $C_u = (2f(x)/(\gamma+1))^{1/2}$, and $C_{2d} = -2\gamma C_{u0}^3/3$, where x_0 and C_{u0} are the steady-state values of x_{s0} and C_u. In Fig. 3, the letters a, b, and c refer to the corresponding cases shown in Fig. 2. In each case only the curves through one saddle point are shown; the repetitive nature of the curves at each saddle point is not shown, for clarity. It should be noted that the value t_0 in Fig. 3, referring to the location of a saddle point, is different for each case. The centers, which also occur at different values of t for each case, are noted in Fig. 3. With the parameters just given, it was found that for the special case shown in Fig. 2b, the special value for G_0 was, from Eq. (23), $(G_0)_{sp} = 4.33$ and from Eq. (26c), $(G_0)_{sp} = 4.77$. The value which gives accurate results (Fig. 3) is:

$$(G_0)_{sp} = 4.968 \tag{27}$$

Thus, Eq. (26c) is helpful in giving a relatively accurate (4% error) first guess for $(G_0)_{sp}$; in another case, with all other parameters the same, but with $x_0 = 0.75$, it was found that Eq. (26c) gave an estimate with an error of 6%. The curves labeled a and c in Fig. 3 were calculated using $G_0 = 5.5 > (G_0)_{sp}$ and $G_0 = 4 < (G_0)_{sp}$, respectively. In each of these cases, curves entering and leaving the saddle point at $t - t_0 = 0$ are shown, the behavior in each case following that sketched in the corresponding part of Fig. 2. The solutions shown in Fig. 3

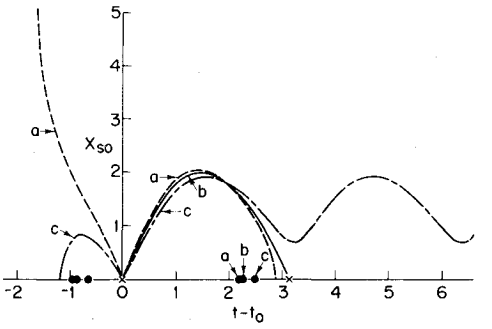

Fig. 3 Calculated integral curves for the simple case represented by Eqs. (15, 18a, 26, and 20a), with $b = 2$, $k = 1$, $a = (\gamma+1)/2 = 1.2$, $x_0 = 1.5$, and $C_{2d} = -2\gamma C_{u0}^3/3$, illustrating the three cases sketched in Fig. 2; curves labeled a (---), b(——), and c (-·—·-) refer to the corresponding cases in Fig. 2. x_0 is the steady-state value of x_{s0}; •, center; x, saddle point.

are for very simple (parabolic) wall shapes. There appears to be no simple way of predicting $(G_0)_{sp}$ for more complicated wall shapes; in general, it is necessary to integrate numerically along an integral curve leaving a saddle point to see which case occurs for the given parameters. Examples are shown later.

With the mathematical behavior of the integral curves through the saddle points understood, it is possible to interpret the physical behavior of the shock wave associated with each of the cases a, b, or c in Fig. 2. First, it is convenient to note those conditions under which a shock wave first must form at the throat as the plenum pressure decreases in a completely subsonic channel flow. This may be done by writing the pressure at $x = X$ using Eqs. (4c, 5b, and 8a) with $t_\ell = 0$; for $f''(X) = 0$, the back or plenum pressure P_b is

$$P_b = 1 - \epsilon\gamma u_1(X) + \epsilon^2\gamma\left[\left(\frac{2\gamma-3}{6}\right)u_1^2(X) - \frac{C_{2d} + G(t)}{u_1(X)}\right] + \ldots \tag{28}$$

where $u_1(X) < 0$. From Eq. (28) and a similar equation written at $x = 0$, it is seen that the condition for the back pressure to be that which gives the subsonic solution for $0 < x < X$ with sonic pressure at the throat is:

$$C_{2d} + G(t) = 0 \tag{29}$$

But this condition, for the case where $G(t)$ (and hence the pressure) is decreasing, is precisely the condition for the saddle point, as exemplified by Eqs. (15) and (16) and the discussion following these equations. As the back pressure decreases, such that $C_{2d} + G(t) < 0$, then a shock wave must be formed at the throat immediately, since there is no time lag between the plenum and channel pressures, and then move downstream. Thus, the integral curve leaving the saddle point is the solution which corresponds to the physical behavior of the shock wave as it forms at the throat and moves downstream. With this fact in mind, one can categorize the possible shock-wave motions associated with each of the cases a, b, and c, in Fig. 2; which of these cases occurs depends on G, $f(x)$, x_0, and k, as mentioned previously. In the following, the term "initial condition" refers to the initial shock-wave location, i.e., the steady-state shock location before the back pressure begins to oscillate.

In Fig. 2a, one can see that for any initial condition which does not lie on an integral curve entering a saddle point (two are illustrated by circles in Fig. 2a; the subsequent shock motion is shown by the dashed lines through these circles), the shock passes through the throat and disappears upstream. Thereafter, the flow in the channel is everywhere subsonic until a saddle point occurs at $x_{s0} = 0$, at which point a shock wave forms at the throat and follows the path indicated by the

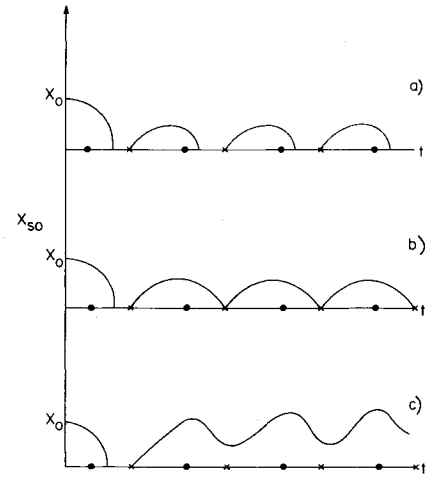

Fig. 4 Sketches of shock-wave motion when the amplitude of the impressed pressure oscillation is large enough to drive the shock wave upstream of the throat, for each of the three cases shown in Fig. 2; cases labeled a, b, and c refer to the corresponding cases in Fig. 2. x_0 is the initial, steady-state condition for the shock position.

integral curve leaving the saddle point; i.e., it travels downstream, then moves back upstream and disappears, forming at the throat again at the time associated with the next saddle point, etc. Thus, no matter what the initial condition is, the final shock motion is described by the integral curves leaving the saddle points as shown in Fig. 4a. For the periods of time between the disappearance and appearance of a shock wave, the flow is subsonic throughout the channel. If the initial condition corresponds to a point on an integral curve entering the saddle point, the shock moves to the throat and then downstream of the throat on the integral curve leaving the saddle point. Thereafter, its motion is the same as that shown in Fig. 4a.

Referring now to the dividing case shown in Fig. 2b, it is seen that there are several different possibilities for the shock motion depending on the initial condition, again indicated by circles. If the initial condition lies outside the integral curves through the saddle points, the shock position merely oscillates with time, never going through the throat. If the initial condition lies beneath the integral curves through the saddle points, the shock moves upstream, passes through the throat and disappears; it then forms at the throat at the time corresponding to the first saddle point after its disappearance. Then it follows the integral curves through the saddle points, so that thereafter it just moves to the throat and never passes upstream; this motion is illustrated in Fig. 4b. If the initial condition should lie on an integral curve through a saddle point, the shock position is completely described by integral curves through the saddle points; the shock never moves upstream of the throat.

Finally, referring to Fig. 2c, there are again several possible initial conditions. If the initial condition lies above the integral curve entering the saddle point, the shock motion approaches a periodic form, never reaching the throat. If it lies on an integral curve below the curve entering the saddle point, it moves upstream through the throat and disappears, forms at the throat at the time corresponding to the first saddle point after its disappearance, and then moves away from the throat and approaches a periodic motion, never approaching the throat again. This motion is shown in Fig. 4c. Finally, if the initial condition should lie on the integral curve entering the saddle, the shock wave moves to the throat, moves away immediately on the integral curve leaving the saddle point, and approaches the same periodic motion previously mentioned.

The numerical examples shown thus far (e.g., Fig. 3) have been for simple wall geometries for which it is possible to

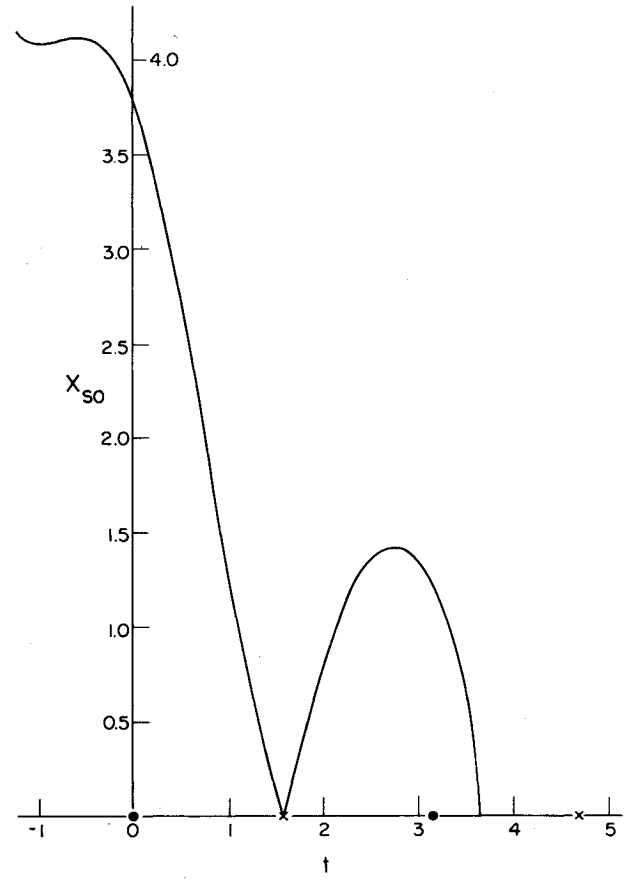

Fig. 5 Calculated integral curves through the saddle point illustrating the case sketched in Fig. 2a for $C_{2d}=0$, $G=4\sin 2t$, $\gamma=1.4$, $\tau=100$, $\epsilon=0.1$, $C_w=0$, and $f(x)$ as given in Eq. (30). Solutions are found by numerically integrating Eq. (11).

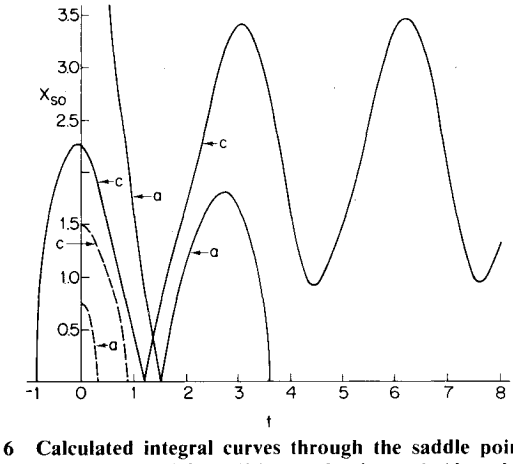

Fig. 6 Calculated integral curves through the saddle points (solid lines) and from the initial condition to the time axis (dotted lines) for two values of x_0 and thus C_{2d}. For curves marked a, corresponding to the case sketched in Fig. 2a, $x_0=1.5$; for curves marked c, corresponding to the case sketched in Fig. 2c, $x_0=0.75$. For each case, $G=4.5\sin 2t$, $\gamma=1.4$, $\tau=150$, $\epsilon=0.1$, $C_w=0$, and $f(x)$ is as given in Eq. (30).

derive an approximate relationship between the parameters for the special dividing case shown in Fig. 2 [Eq. (26c)]. For general geometries, it is necessary to integrate Eq. (11) numerically along the integral curve leaving the singularity, using Eq. (17a) to find starting values near $x_{s0}=0$, to find which case holds. Examples of such calculations, for more complicated wall shapes, are shown in Figs. 5 and 6. In these

calculations, $f(x)$ is:

$$f(x) = 18x^2/13 \qquad x<1$$
$$= 27(x-2)^4/13 + 48(x-2)^3/13 + 3 \qquad 1 \le x \le 2$$
$$= 3 \qquad x>2 \qquad (30)$$

Figure 5 shows calculations made for $C_{2d}=0$, that is, for the case where the steady-state solution is that for which the flow goes through sonic velocity at the throat but is subsonic thereafter, with no shock waves. Clearly, the unsteady motion is that illustrated in Fig. 2a. In Fig. 6, two examples are shown in which the only parameter varied is the steady-state shock position, x_0. Referring to the integral curves through the first saddle points, it is seen that for $x_0 = 1.5$ the situation is that illustrated in Fig. 2c while for $x_0 = 0.75$ it is that illustrated in Fig. 2a. Also shown in Fig. 6 are the solution curves from the initial condition to the point where the shock passes through the throat. With these two curves and those leaving the first saddle point, one can then find the resulting shock wave motions corresponding to Figs. 4a ($x_0 = 0.75$) and 4c ($x_0 = 1.5$).

Conclusions

For general channel wall shapes, the shock-wave motion associated with an oscillating back pressure is found by integrating Eq. (11) numerically. In the event that conditions are such that the shock wave moves upstream through the throat and disappears, the subsequent shock motion may be found by integrating Eq. (11) along the integral curves leaving the saddle point, using Eq. (17a) for starting values. This integration will establish which of the cases illustrated in Fig. 4a exists for the given conditions and this will allow prediction of the subsequent shock-wave motion.

The previous examples illustrate the remarkably varied shock-wave motions governed by the simple first-order nonlinear Eq. (11). Moreover, they illustrate the well-known fact that in transonic channel flows, small changes in downstream pressures can cause large local changes in pressure by changing the location of the shock; in these examples, the pressure jump across the shock is $O(\epsilon)$, and the position is governed by changes in back pressure $O(\epsilon^2)$. Finally, they show that large changes in shock position can result from small changes in back pressure; i.e., for $\Delta P_b = O(\epsilon^2)$, $\Delta x_s = O(1)$. The solutions presented allow relatively simple calculations of shock positions to be made for transonic flows in symmetric channels with arbitrary wall shapes and arbitrary oscillations in back pressure. The extension to asymmetric channels, still with radius of curvature $O(\epsilon^{-2})$ is not difficult, and it appears that these results may have application to inlet buzz and to flutter problems in turbomachinery.

It may be noted that according to Eq. (11), when the shock wave passes through the throat moving upstream, it does so with an infinite velocity. This simply indicates that the expression for the shock-wave velocity is not uniformly valid in the region of the throat, so that an inner region must be considered there in which corrections to the shock-wave velocity may be calculated. As shown in the Appendix, the corrected shock-wave velocity is finite, but now of order $\epsilon^{3/2}$ rather than ϵ^2, and the jump in pressure across the shock as it passes through the throat is $O(\epsilon^{3/2})$ rather than $O(\epsilon)$.

Appendix

When the shock wave is moving upstream and approaching the throat, the solutions are not uniformly valid, as indicated, for example, by the fact that the shock-wave velocity and fluid velocity approach infinite values. The manner in which corrections to the solutions are found may be illustrated for a given wall shape in the neighborhood of the channel throat; here the often-used parabolic shape, Eq. (18a), is employed. Then, when the shock wave is near the throat, the velocity downstream of the throat is, from Eqs. (4, 5, and 8a) with $t_l = 0$,

$$u = 1 - \epsilon\sqrt{\frac{2a}{\gamma+1}}\,x + \epsilon^2\left\{a\left(y^2 - \frac{1}{3}\right) - \frac{(2\gamma-3)}{3(\gamma+1)}\,ax^2 - \sqrt{\frac{\gamma+1}{2a}}\,\frac{(C_{2d}+G(t))}{x} + \xi_x^{**}\right\} + \ldots \qquad (A1)$$

Thus, for $C_{2d} + G(t) \neq 0$, it is seen that when $x = O(\epsilon^{1/2})$, the first- and second-order terms become of the same order, and an inner region must be considered, of order $\epsilon^{1/2}$ in thickness. In this region, then, a new coordinate $\tilde{x}$ is defined, such that:

$$\tilde{x} = x/\epsilon^{1/2} \qquad (A2)$$

and so Eq. (A1) may be written as:

$$u = 1 - \epsilon^{3/2}\left\{\sqrt{\frac{2a}{\gamma+1}}\,\tilde{x} + \sqrt{\frac{\gamma+1}{2a}}\,(C_{2d}+G(t))/\tilde{x}\right\} + \epsilon^2 a\left(y^2 - \frac{1}{3}\right) - \epsilon^3\,\frac{(2\gamma-3)}{3(\gamma+1)}\,a\tilde{x}^2 + \ldots \qquad (A3)$$

where t is defined in Eqs. (2) and (3).

In the same way, one can use Eqs. (9) and (10) to write the corresponding equations for the shock-wave velocity:

$$u_s = -\epsilon^{3/2}\left(\frac{\gamma+1}{4}\right)\sqrt{\frac{\gamma+1}{2a}}\,(C_{2d}+G(t))/\tilde{x}_s + \ldots \qquad (A4)$$

Equations (A3) and (A4) are the outer solutions to which the inner solutions must match term by term.

In the inner region, it is seen from Eq. (A3) that $u = 1 + O(\epsilon^{3/2})$. One can define a velocity potential ϕ to the order desired, where $u = \phi_x = \epsilon^{-1/2}\phi_{\tilde{x}}$ and $v = \phi_y$. The expansion for ϕ is:

$$\phi = \epsilon^{1/2}\tilde{x} + \epsilon^2\tilde{\phi}_1(\tilde{x},y,t) + \epsilon^{5/2}\tilde{\phi}_2(\tilde{x},y,t) + \epsilon^2\tilde{\phi}_3(\tilde{x},y,t) + \ldots \qquad (A5)$$

The wall boundary conditions are found by expanding Eq. (1) about $x = 0$, writing the resulting equation in terms of $\tilde{x}$ and requiring that the flow be tangent to the walls. Then,

$$\tilde{\phi}_{1y}(\tilde{x}, \pm 1, t) = 0 \qquad (A6)$$

$$\tilde{\phi}_{2y}(\tilde{x}, \pm 1, t) = \pm 2a\tilde{x} \qquad (A7)$$

$$\tilde{\phi}_{3y}(\tilde{x}, \pm 1, t) = 0 \qquad (A8)$$

Finally, the jump conditions across the shock wave are written relative to the moving shock wave.[1,2] Since, from Eq. (A4), it is seen that $u_s = O(\epsilon^{3/2})$ in the inner region, the general expansions for the shock-wave velocity and the jump conditions are:

$$u_s = \epsilon^{3/2}\tilde{u}_{s0}(t) + \ldots \qquad (A9)$$

$$(u_u - u_s)(u_d - u_s) = 1 - 2\left(\frac{\gamma-1}{\gamma+1}\right)\epsilon^{3/2}\tilde{u}_{s0} + \ldots \qquad (A10)$$

If Eqs. (A2) and (A5) are substituted into the potential equation, linear governing equations for each of the $\tilde{\phi}_i$ are obtained. These equations are easily integrated and, after applying the boundary conditions, Eqs. (A6-A9), one finds

that for $x>x_s$,

$$\tilde{\phi}_{1\tilde{x}} = -\sqrt{\frac{2a}{\gamma+1}\tilde{x}^2 + \tilde{C}_1(t)} \tag{A11}$$

$$\tilde{\phi}_{2\tilde{x}} = a\left(y^2 - \frac{1}{3}\right) + \frac{\tilde{M}(t)}{\tilde{\phi}_{1\tilde{x}}} \tag{A12}$$

where $\tilde{C}_1(t)$ and $\tilde{M}(t)$ are functions of integration. These solutions are used to write the inner solutions for u, and the resulting equation is written for $\tilde{x}\gg 1$ and compared with Eq. (A3). Then for the solutions to match, it is found that for $x>x_s$

$$\tilde{C}_1(t) = 2[C_{2d} + G(t)] \tag{A13}$$

$$\tilde{M}(t) = 0 \tag{A14}$$

Upstream of the shock wave $\tilde{\phi}_{1\tilde{x}}>0$; $\tilde{C}_1=0$ and $\tilde{M}=0$ since the flow is sonic at the throat. With $\tilde{\phi}_{1\tilde{x}}$ known upstream and downstream of the shock, one can use Eqs. (A9) and (A10) to show that the shock-wave velocity in the inner region is:

$$\tilde{u}_{s0} = -\left(\frac{\gamma+1}{4}\right)\left[\sqrt{\frac{2a}{(\gamma+1)}\tilde{x}_s^2 + \tilde{C}_1(t)} - \sqrt{\frac{2a}{\gamma+1}}\tilde{x}_s\right] \tag{A15}$$

For $\tilde{x}\gg 1$, and $\tilde{C}_1$ as given in Eq. (A13), the inner shock-wave velocity, Eqs. (A9) and (A15), matches with the outer shock velocity, Eq. (A9), as it should.

Finally, by adding the inner and outer solutions and substracting the common terms (those used in matching), one can write composite solutions for u_s and u for $x>x_s$, uniformly valid to order $\epsilon^{3/2}$ throughout the channel. Thus,

$$\begin{aligned} u = 1 &+ \epsilon\left\{u_1 - \sqrt{\frac{2a}{\gamma+1}x^2 + 2\epsilon[C_{2d}+G(t)]} + \sqrt{\frac{2a}{\gamma+1}}x\right\} \\ &+ \epsilon^2\left\{\frac{f''}{2}\left(y^2 - \frac{1}{3}\right) - (2\gamma-3)u_1^2/6 + \zeta_x^{**}\right. \\ &\left. + [C_{2d}+G(t)]\left(\frac{1}{u_1} + \sqrt{\frac{\gamma+1}{2a}}\frac{1}{x}\right)\right\} + \ldots \quad x>x_s \end{aligned} \tag{A16}$$

$$\begin{aligned} u_s = &-\epsilon\frac{(\gamma+1)}{4}\left\{\sqrt{\frac{2a}{\gamma+1}x_s^2 + 2\epsilon[C_{2d}+G(t)]}\right. \\ &\left. - \sqrt{\frac{2a}{\gamma+1}}x_s\right\} + \epsilon^2\left(\frac{\gamma+1}{4}\right)\left\{\left(\frac{1}{u_{1u}}\right.\right. \\ &\left.\left. - \sqrt{\frac{\gamma+1}{2a}}\frac{1}{x_s}\right)\left(C_{2d}+G(t)\right) + \frac{2\gamma}{3}u_{1u}^2\right\} + \ldots \end{aligned} \tag{A17}$$

It is seen that as $x\to 0$, u_s and u remain finite. It should be noted that the solutions represented by Eqs. (A16) and (A17) are necessary only for $C_{2d}+G(t)\geq 0$, i.e., for the case where the shock wave is approaching the throat from downstream or when subsonic flow exists throughout the channel. As soon as $C_{2d}+G(t)$ becomes negative, corresponding to the shock wave forming at the throat and moving downstream, the shock velocity and flow velocity downstream of the shock are finite and no inner solutions are necessary. The outer solutions, as presented in the text, are valid to the order indicated.

Acknowledgment

This work was partially supported by Naval Air Systems Command under Contract N0019-76-C-0435. This support is gratefully acknowledged.

References

[1] Richey, G. K. and Adamson, Jr., T. C., "Analysis of Unsteady Transonic Channel Flow with Shock Waves," *AIAA Journal*, Vol. 14, Aug. 1976, pp. 1054-1061.

[2] Chan, J. S.-K. and Adamson, Jr., T. C., "Unsteady Transonic Flows with Shock Waves in an Asymmetric Channel," *AIAA Journal*, Vol. 16, April 1978, pp. 377-384.

[3] Messiter, A. F. and Adamson, Jr., T. C., "Asymptotic Solutions for Nonsteady Transonic Channel Flows," *Symposium Transsonicum II*, edited by K. Oswatitsch and D. Rues, Springer-Verlag, 1976, pp. 41-48.

[4] Adamson, Jr., T. C. and Liou, M. S., "Unsteady Motion of Shock Waves in Two Dimensional Transonic Channel Flows," Rept. UM 014534-F, June 1977.

[5] Messiter, A. F. and Adamson, Jr., T. C., "On the Flow Near a Weak Shock Wave Downstream of a Nozzle Throat," *Journal of Fluid Mechanics*, Vol. 69, 1975, pp. 97-108.